Combining a root exclusion technique with continuous chamber and porous tube measurements for a pin-point separation of ecosystem respiration in croplands

Mathias Hoffmann[1]*, Stephan J. Wirth[2], Holger Beßler[3], Christof Engels[3], Hubert Jochheim[4], Michael Sommer[1, 5], and **Jürgen Augustin[2]**

[1] Leibniz Centre for Agricultural Landscape Research (ZALF), Institute of Soil Landscape Research, 15374 Müncheberg, Germany
[2] Leibniz Centre for Agricultural Landscape Research (ZALF), Institute of Landscape Biogeochemistry, 15374 Müncheberg, Germany
[3] Humboldt University Berlin, Albrecht-Daniel-Thaer Institute of Agricultural and Horticultural Sciences, 10115 Berlin, Germany
[4] Leibniz Centre for Agricultural Landscape Research (ZALF), Institute of Landscape Systems Analysis, 15374 Müncheberg, Germany
[5] University of Potsdam, Institute of Earth and Environmental Sciences, 14476 Potsdam, Germany

Abstract

To better assess ecosystem C budgets of croplands and understand their potential response to climate and management changes, detailed information on the mechanisms and environmental controls driving the individual C flux components are needed. This accounts in particular for the ecosystem respiration (R_{eco}) and its components, the autotrophic (R_a) and heterotrophic respiration (R_h) which vary tremendously in time and space. This study presents a method to separate R_{eco} into R_a [as the sum of $R_{a\ (shoot)}$ and $R_{a\ (root)}$] and R_h in order to detect temporal and small-scale spatial dynamics within their relative contribution to overall R_{eco}. Thus, predominant environmental drivers and underlying mechanisms can be revealed.

R_{eco} was derived during nighttime by automatic chamber CO_2 flux measurements on plant covered plots. R_h was derived from CO_2 efflux measurements, which were performed in parallel to R_{eco} measurements on a fallow plot using CO_2 sampling tubes in 10 cm soil depth. $R_{a\ (root)}$ was calculated as the difference between sampling tube CO_2 efflux measurements on a plant covered plot and R_h. $R_{a\ (shoot)}$ was calculated as $R_{eco} - R_{a\ (root)} - R_h$. Measurements were carried out for winter wheat (*Triticum aestivum* L.) during the crop season 2015 at an experimental plot located in the hummocky ground moraine landscape of NE Germany. R_{eco} varied seasonally from < 1 to 9.5 g C m^{-2} d^{-1}, and was higher in adult (a) and reproductive (r) than juvenile (j) stands (g C m^{-2} d^{-1}: j = 1.2, a = 4.6, r = 5.3). Observed R_a and R_h were in general smaller compared to the independently measured R_{eco}, contributing in average 58% and 42% to R_{eco}. However, both varied strongly regarding their environmental drivers and particular contribution throughout the study period, following the seasonal development of soil temperature and moisture (R_h) as well as crop development (R_a). Thus, our results consistently revealed temporal dynamics regarding the relative contribution of $R_{a\ (root)}$ and $R_{a\ (shoot)}$ to R_a, as well as of R_a and R_h to R_{eco}. Based on the observed results, implications for partitioning of R_{eco} in croplands are given.

Key words: automatic chambers / autotrophic respiration / heterotrophic respiration / soil CO_2 sampling tubes

Accepted July 02, 2017

1 Introduction

At a global scale, soils are storing two to three times as much carbon (C) as the atmosphere and biosphere, respectively (*Batjes*, 1996; *Lal* et al., 2004; *Chen* et al., 2015). Consequently, detecting changes in soil organic carbon (ΔSOC) stocks is of considerable interest when investigating the C cycle of terrestrial ecosystems. Moreover, growing interest has been recently paid on the influence of human activities on the C budget of croplands, which cover ≈ 1.400 Mha worldwide and store up to ≈ 248 Pg C (*Eglin* et al., 2010). It is assumed that especially tillage erosion might yield in additional C sequestration and, thus, contribute to the missing terrestrial carbon sink (*Van Oost* et al., 2007). However, due to the high spatial and temporal dynamics and magnitudes of single C fluxes, the particular influence of human activities, underlying mechanisms and environmental variables driving ΔSOC of croplands are still unclear (*Lugato* et al., 2014; *Luo* et al., 2015). Compared to repeated soil inventories, which are often conducted during long-term field trials (*Schrumpf* et al., 2011; *Batjes* and *van Wesemael*, 2015; *Chen* et al., 2015), measurements of all relevant C fluxes might be used as a more precise method to calculate spatial and temporal dynamics of the net ecosystem carbon balance (NECB; *Smith* et al., 2010) and, thus, estimates of ΔSOC (*Hoffmann* et al., 2017). Nevertheless, a precise and accurate determination of NECB is complicated. Only minor changes in one of the extensive and opposing C fluxes, forming the NECB, such as ecosystem

* Correspondence: M. Hoffmann; e-mail: mathias.hoffmann@zalf.de

© 2018 WILEY-VCH Verlag GmbH & Co. KGaA, Weinheim

respiration (R_{eco}) or gross primary productivity (GPP), may cause a major change in the rather small values of net ecosystem exchange (NEE) as well as the final NECB. Compared to other components of the C budget and despite of recent developments in measurement techniques, especially measurements of R_{eco}, are related to a high uncertainty (*Bond-Lamberty* et al., 2004; *Zhang* et al., 2013). Reasons for this are methodological limitations regarding the separation of R_{eco} into its autotrophic (R_a; sum of root and shoot respiration by autotrophic plants) and heterotrophic (R_h; respiration of soil organisms due to the decomposition of organic material) respiration components. Therefore, it is crucial to separate the R_{eco} flux and gain detailed information on the mechanisms and environmental drivers that control R_a (sum and components) and R_h to improve estimates of R_{eco}. This will help to improve ΔSOC estimates for croplands and to understand its potential response to climate and management changes. Different *in situ* and *in vitro* approaches as well as combinations of measurement techniques in order to separate R_{eco} into R_a and R_h, including root exclusion, physical separation of components, isotopic techniques, and modelling based approaches were compared and evaluated in a number of studies (*Hanson* et al., 2000; *Kuzyakov* and *Larionova*, 2005; *Subke* et al., 2006). Out of these, especially root exclusion techniques, such as tree-girdling in forest ecosystems (*Bhupinderpal-Singh* et al., 2003) and root removal and trenching in grassland and cropland ecosystems (*Suleau* et al., 2011) were used in recent field studies (*Suleau* et al., 2011; *Zhang* et al., 2013; *Prolingheuer* et al., 2014; *Demyan* et al., 2016). Compared to forest or perennial ecosystems, root exclusion methods are easy to implement in croplands by not sowing or regularly weeding the fallow plot (*e.g.*, *Suleau* et al., 2011).

However, in most of these studies an eddy covariance system was used to measure R_{eco}, whereas R_h was obtained on a fallow plot within the footprint area using manual or automatic chamber systems (*Suleau* et al., 2011; *Zhang* et al., 2013; *Demyan* et al., 2016). Thus, R_{eco} flux separation was performed by subtracting spatially distinct point measurements of R_h from spatially integrated R_{eco} fluxes, resulting from the eddy covariance (EC) footprint area. This might introduce a bias due to small-scale spatial heterogeneity of root and heterotrophic respiration as reported, *e.g.*, by *Prolingheuer* et al. (2014). Moreover, R_{eco} flux measurements might be biased to a lower extend, since they do not exclude emissions from the fallow plot, where only R_h fluxes occur. To perform flux partitioning of R_{eco} into R_h and R_a on a smaller spatial scale (several cm^2 to few m^2), we combined a root exclusion experimental setup with continuous CO_2 flux measurements using big-sized automatic chambers and soil CO_2 sampling tubes. Thus, we were able not only to detect the soil CO_2 efflux {soil tubes; used to separate R_a into its below [$R_{a\ (root)}$] and aboveground [$R_{a\ (shoot)}$] components} but also overall R_{eco} (automatic chambers). Measurements were performed at the hummocky ground moraine landscape of NE Germany, which is characterized by distinct small-scale soil heterogeneity. We hypothesize that the presented approach based on the combination of a root exclusion experimental setup and continuous above and belowground CO_2 concentration measurements: (1) allows for quantifying the relative contribution of R_a [$R_{a\ (root)}$, $R_{a\ (shoot)}$] and R_h to R_{eco} throughout crop development, and (2) helps to identify environmental drivers for R_a [$R_{a\ (root)}$, $R_{a\ (shoot)}$] as well as R_h. For this purpose we analyzed temporal dynamics of R_{eco}, separated into its components R_a [$R_{a\ (root)}$, $R_{a\ (shoot)}$] and R_h for winter wheat (*Triticum aestivum* L.) during an entire crop season.

2 Material and methods

2.1 Study site and experimental setup

Measurements were carried out for winter wheat (*Triticum aestivum* L.) from November 2014 to end of July 2015 at a topographic depression on the 6 ha large experimental field "CarboZALF-D" (plot 10; *Sommer* et al., 2016). The site is located in a hummocky arable soil landscape of the Uckermark region (NE-Germany; 53°23′N, 13°47′E, ≈ 50–60 m asl). The temperate climate is characterized by a mean annual temperature of 8.6°C and annual precipitation of 498 mm (1992–2012, ZALF research station Dedelow). The study site shows complex soil patterns mainly influenced by erosion, topography, and parent material, *e.g.*, sandy to marly glacial and glaciofluvial deposits. The soil studied is classified as an Endogleyic Colluvic Regosols (Eutric) overlying peat (*IUSS Working Group WRB*, 2015), influenced by a fluctuating ground water level (GWL). Throughout the study period the site was solely mineral fertilized and treated according to the general farming practice of the surrounding area.

R_{eco} was derived from CO_2 flux measurements from plant stand and soil during nighttime using automatic chambers. The chambers used are part of the CarboZALF experimental setup, in which four automatic chambers were arranged along a topographic gradient (upper, upper middle, lower middle, lower slope position; length 30 m; difference in altitude ≈ 1 m) in a distance of approximately 5 m to each other (*Sommer* et al., 2016). For the purpose of this study, only measurements of the two lowermost chambers were considered. To avoid mutual interference of chamber and soil tube based CO_2-flux estimates, average CO_2-fluxes measured by two automatic chambers framing the soil tube measurement plots were used (Fig. 1). Thus, the influence of small-scale soil heterogeneity on separated flux components was assumed to be minimized. Flux separation of R_{eco} into R_h and R_a is based on a root exclusion experimental setup and measurements of belowground soil CO_2 concentrations, using two soil CO_2 sampling tubes installed at a plot covered with wheat and a fallow plot, respectively (Fig. 1). Therefore, two neighboring square trenches (each 1 m length, 20 cm width, 30 cm depth) in between the two lower automatic chambers were excavated during early October 2014. One of both square trenches was coated with wire cloth (35 μm mesh size) towards the outward soil, thus, providing a fallow plot allowing for R_h measurements. Whereas R_h was derived directly from nighttime measurements performed at the fallow plot [$R_h = R_{(fallow\ plot)}$], R_a was calculated as the difference between nighttime measurements of R_{eco} and R_h ($R_a = R_{eco} - R_h$) (Fig. 1). R_a was further separated into shoot [$R_{a\ (shoot)}$] and root respiration [$R_{a\ (root)}$]. To obtain $R_{a\ (shoot)}$, the measured soil respiration at the wheat-covered CO_2 sampling plot (R_{soil}) was subtracted

© 2018 WILEY-VCH Verlag GmbH & Co. KGaA, Weinheim

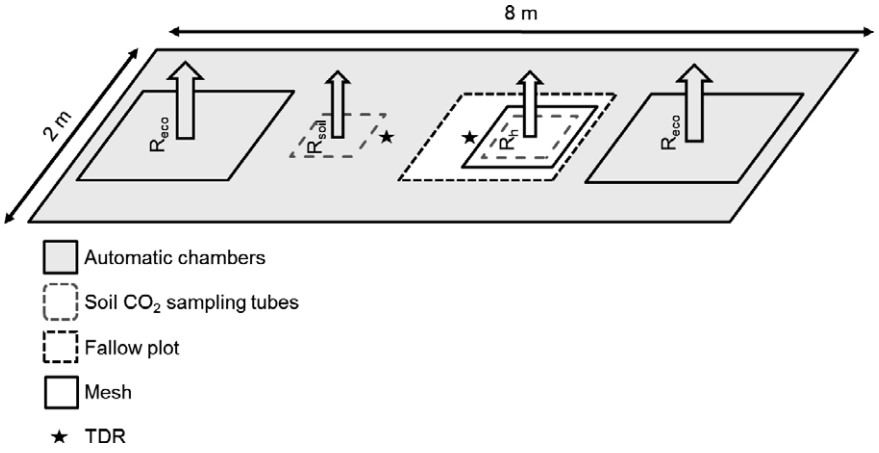

Figure 1: Schematic representation of the experimental setup.

from R_{eco} [$R_{a\ (shoot)} = R_{eco} - R_{soil}$]. $R_{a\ (root)}$ was calculated as the difference between R_{soil} and R_h [$R_{a\ (root)} = R_{soil} - R_h$].

Records of meteorological conditions (1 min frequency) included air temperature in 20 cm and 200 cm height, PAR (photosynthetic active radiation; inside and outside the chamber; SKP 215, Skye Instruments Ltd, Llandrindod Wells, UK), air humidity, precipitation, air pressure, wind speed and direction (WXT520 weather transmitter, Vaisala, Helsinki, Finland). Soil temperatures were recorded next to the climate station (107, Campbell Scientific, Logan, USA) in 2, 5, 10, and 50 cm soil depth using thermocouples. In addition, soil moisture and soil temperature in 10 cm depth were monitored next to the square trenches by TDR probes (TRIME-pico 64, IMKO GmbH, Ettlingen, Germany) in 30 min intervals.

2.2 Chamber CO_2 flux determination

2.2.1 Automatic chamber system

The automatic flow-through non-steady-state (FT-NSS) closed chamber (AC) (*Livingston* and *Hutchinson*, 1995) system is described in detail in *Hoffmann* et al. (2017). Chambers were made of identical, rectangular, transparent polycarbonate cubes (thickness of 2 mm; light transmission of ≈ 70%). Each chamber had a height of 1.5 m and covered a surface area of 2.25 m^2 (volume: 3.38 m^3). Airtight closure during measurements was ensured by a rubber belt sealing at the bottom of each chamber. A 30 cm open-ended tube on the slightly concavely arched top of the chambers passed collected rain water into the chamber and assured equilibration of possible air pressure deficits during the measurement. Two small axial fans (5.61 $m^3\ min^{-1}$) were used for mixing the chamber headspace. The chambers are mounted onto steel frames with a height of 6 m and lifted in between measurements by electrical winches at the top. For controlling the AC system and data collection, a CR1000 data logger was used (Campbell Scientific, UT, USA). For easy access, the data logger was connected to a GSM-modem. Data logger and controlling device were placed inside a weathering-sheltered hut next to the measurement site. CO_2 concentration changes over time were measured within each chamber by a carbon dioxide probe (GMP343, Vaisala, Helsinki, Finland) connected to a vacuum-pump (1 L min^{-1}; DC12/16FK, Fürgut, Tannheim, Germany). All CO_2 probes were calibrated prior to installation by using ± 0.5% accurate gases, containing 0, 200, 370, 600, 1000, and 4000 ppm CO_2. Chambers closed in parallel at an hourly frequency, providing one flux measurement per chamber and hour. Nighttime measurements usually lasted for 10 min during the growing season and 20 min during the non-growing season. CO_2 concentrations (inside the chamber) and general environmental conditions, such as PAR (SKP215, Skye, Llandridad Wells, UK) and air temperatures (107, Campbell Scientific, UT, USA), were recorded inside and outside the chamber in a 15 sec interval.

2.2.2 Flux calculation

An adaptation of the modular R program script, described in detail by *Hoffmann* et al. (2015) was used for stepwise data processing. Based on records of CO_2 concentration change within chamber headspace and environmental variables, CO_2 fluxes were calculated and parameterized for ecosystem respiration (R_{eco}; nighttime measurements) and gross primary production (GPP; based on NEE daytime measurements) within one integrative step. For this study only nighttime R_{eco} measurements are shown. Automatic chamber CO_2 flux rates ($\mu g\ m^{-2}\ s^{-1}$) were calculated according to the ideal gas law Eq. (1):

$$CO_{2_{Reco}} = \frac{M \times P \times V \times \delta v}{R \times T \times t \times A}, \quad (1)$$

by using base area (A), within-chamber air temperature (T), air pressure (P), the constant R (8.3143 m^3 Pa K^{-1} mol^{-1}), and chamber volume (V). Since plants below the chambers accounted for only < 0.2% of the total chamber volume, a static chamber volume was assumed. The CO_2 concentration change (δv) over measurement time (t), was calculated by applying a linear regression (*Leiber-Sauheitl* et al., 2014; *Pohl* et al., 2015), which estimates the flux by using the least squares method, to data subsets based on a variable moving window with a minimum length of 4 min (*Hoffmann* et al., 2015). To exclude data noise originating from turbulences and pressure fluctuation caused by chamber deployment or from increasing saturation and canopy microclimate effects (*Kutzbach* et al., 2007; *Langensiepen* et al., 2012) a deathband of 5% was applied prior to moving-window flux calculation. Thus, derived numerous possible CO_2 fluxes per measurement were further evaluated according to the following inclusion criteria: (1) a range (minimum to maximum) of within-chamber air temperature not larger than ± 1.5 K (R_{eco} and NEE) and a deviation of PAR not larger than ± 20% of the average (NEE only) to ensure stable environmental conditions within the chamber throughout the measurement; (2) a significant regression slope ($p \leq 0.1$, t-statistic); and (3) signifi-

© 2018 WILEY-VCH Verlag GmbH & Co. KGaA, Weinheim

cant tests ($p < 0.1$) for normality (Lillifor's adaption of the Kolmogorov–Smirnov test), homoscedasticity (Breusch–Pagan test) and linearity of CO_2 concentration data. Calculated CO_2 fluxes that do not meet all inclusion criteria were discarded (< 1%). To avoid fluxes affected by saturation (in case of R_{eco}) or limitation (in case of GPP) being taken into account for flux calculation, the CO_2 flux with the steepest slope was chosen out of the remaining fluxes.

2.3 Soil CO_2 sampling tube flux determination

2.3.1 Soil CO_2 concentration measurements

In each of both trenches, a hydrophobic, gas-permeable polypropylene tube (4 m length, 5.5 mm inner diameter, 1.55 mm wall thickness; ACCUREL® PP V8/2HF, Membrana GmbH, Wuppertal, Germany) was buried horizontally at 10 cm soil depth. Both ends of the buried tubes were fitted with pneumatic tubing that was resistant to CO_2 diffusion (eba pneumatic GmbH, Schwaikheim, Germany) and connected to an aboveground instrumentation enclosure. Soil gas that diffused into the inner tubing was circulated *via* a closed-loop into the instrumentation enclosure, driven by peristaltic pumps (Gardner Denver Thomas GmbH, Puchheim, Germany). From the pump, gas was routed to a NDIR sensor (measurement range: 0 to 100,000 μmol mol^{-1}; MSH-P-CO2; Dynament Ltd., South Normanton, UK). Prior to the soil CO_2 concentration measurements performed every 30 min, soil gas was circulated for 90 sec. Data acquisition and controlling of instrumentation was ensured by a data logger (DT85; dataTaker, Thermo Fisher Scientific, Scoresby, Australia).

2.3.2 Flux calculation

Estimates of the CO_2 efflux by simultaneously measuring the air and soil (10 cm depth) CO_2 concentration are based on Fick's Law of Diffusivity, where the flux (CO_2 efflux) represents the diffusion rate from a higher ($CO_{2_{soil}}$) to a lower ($CO_{2_{air}}$) concentration through a porous material (soil) with a certain diffusion coefficient along a specific distance (soil depth; *Dz*). Flux calculation was performed according to Eq. (1), following *Moldrop* et al. (1999)

$$CO_{2efflux} = D_{air} \times \frac{(h - u_v)^{2.9*S}}{h} \times \frac{CO_{2air} - CO_{2soil}}{Dz}, \quad (2)$$

where D_{air} is the diffusivity of CO_2 in free air. D_{air} was calculated according to *Tang* et al. (2005) by $D_{air} = D_{air0} \times (T/T_0)^{1.75} \times (P_0/P)$, where D_{air0} is the reference value 1.47×10^{-5} m^2 s^{-1} (*Jones*, 1992) of D_{air} at T_0 (293.15 K) and P_0 (101300 Pa), and *T* and *P* are the temperature (K) and air pressure (Pa), respectively. *h* is the soil porosity calculated by $h = (r_s - r_b)/r_s$, where r_s is the density of mineral soils (assumed to be 2.65 Mg m^{-3}; *Myklebust* et al., 2008) and r_b refers to soil bulk density (1.63 Mg m^{-3}). The u_v is the volumetric water content, and $2.9 \times S$ is the texture-specific tortuosity coefficient (*Myklebust* et al., 2008). *S* is the percentage of mineral soil > 2 μm (silt and sand content; 0.87) and accounts for the larger tortuosity of soil with a high clay content compared to soil with a higher content of silt and sand. As a result, the texture-specific tortuosity coefficient reaches 2.5, which is in good agreement with 2.6 given by *Myklebust* et al. (2008) and the commonly used 2.5 as stated by *Moldrop* et al. (1999). Undisturbed soil cores (100 cm^3) were taken in three replicates to determine bulk density (r_b). After weighing the soil cores an aliquot was taken from each core and dried at 105°C. Bulk soil samples were air-dried, gently crushed and sieved (2 mm) to obtain the fine-earth fraction (< 2 mm). S was assumed to be constant (0.87) throughout the study period (*Myklebust* et al., 2008). Prior to flux calculation, $CO_{2_{soil}}$ measured in 10 cm soil depth was corrected for variations in temperature and pressure following *Tang* et al. (2005).

To account for the seasonal and diurnal variability of near surface air CO_2 concentrations, $CO_{2_{air}}$ measured by the AC system in between chamber closures was used for flux calculation. However, the effect of a varying $CO_{2_{air}}$ compared to $CO_{2_{soil}}$ on the CO_2 efflux is rather negligible. The reason, therefore, are near surface CO_2 concentrations which only vary from 363 ppm to 796 ppm, whereas measured CO_2 concentrations at a depth of 10 cm varied from 546 ppm during periods of frost to up to 26,094 ppm during the growing season.

2.4 Above and belowground biomass development

Above (NPP_{shoot}) and belowground (NPP_{root}) biomass development was monitored throughout the study period. NPP_{shoot} development was recorded during biomass sampling campaigns (at BBCH 30, 60, and 90; *Lancashire* et al., 1991) and biweekly measurements of the leaf area index (LAI; Sunscan, Delta-T devices Ltd., Cambridge, UK). The influence of plant phenology on R_{eco} and its components was investigated by dividing the winter wheat growing period into a juvenile (j) vegetative stage, an adult (a) vegetative stage, and a reproductive (r) stage. The determination of phenological stages was based on biweekly assessments of plant phenology, following *Lancashire* et al. (1991).

Aboveground litter production and NPP_{root} as the sum of root production and loss were measured from plant emergence to harvest in three plots (0.25 m × 1 m), located inbetween the automatic CO_2-measurement chambers at the lower position of the topographic gradient. Production and loss of roots were measured using transparent root observation tubes (mini-rhizotrons). In each plot, two acrylic glass tubes (0.4 m length × 0.07 m outer diameter) were inserted vertically to 0.3 m soil depth. Tubes were sealed with plastic caps at the bottom and top openings. The tube portion remaining aboveground was covered with reflecting tape to avoid light entrance. Images of the complete soil–tube-interface were captured following tube installation (October 7, 2014), in late autumn (November 27, 2014), spring (April 30, 2015), and at harvest (July 30, 2015) using a 360-degree scanner (CI-600, CID-Bioscience, Camas, WA, USA). On four randomly selected areas (0.04 m × 0.04 m) of the soil–tube-interface, newly produced and lost roots were identified by comparing consecutive images and quantified by counting. Numbers of newly produced and lost roots (n cm^{-2} soil–tube-interface) were multiplied with the ratio of the standing root biomass at harvest (g dry mass m^{-2} soil surface),

© 2018 WILEY-VCH Verlag GmbH & Co. KGaA, Weinheim

quantified by sampling rootstocks in one meter row and fine roots in one soil core (0.065 diameter × 0.3 m depth) per plot, to the number of roots present along the soil–tube-interface at harvest (n cm^{-2}), to derive the biomass of the newly produced and lost roots (g m^{-2}). Aboveground litter production was measured by collecting litter and senescent leaves on an area of 0.25 m × 1 m per plot at the mini-rhizotron sampling dates.

2,5 Statistical analyses

CO_2 fluxes measured above (AC system; R_{eco}) and belowground (soil CO_2 concentration measurement system; R_h and R_{soil}) were tested for normal distribution and variance homogeneity, using the Kolmogorow–Smirnow and Levene's test, respectively. Since the data sets showed normal distribution and variance homogeneity, the parametric pairwise t-test was used to check whether the R_{eco} components R_h and R_a were significantly lower ($p < 0.05$) compared to measured R_{eco} fluxes using the AC system. The test was performed for fluxes measured during the juvenile (j), adult (a) and reproductive (r) plant phenological stages to determine the influence of plant development on the contribution of the different fluxes on R_{eco}. Analyses were carried out using the statistical software R (R 3.1.0).

3 Results and discussion

3.1 Automatic chamber and soil tube derived CO_2 fluxes – dynamics and drivers

Average seasonal R_{eco} and its components R_h, $R_{a\ (root)}$, and $R_{a\ (shoot)}$ for the juvenile, adult, and reproductive plant development stage, as well as the corresponding average soil temperatures, above and belowground biomass development and precipitation are presented in Tab. 1. With an average flux of 1.54 g C m^{-2} d^{-1}, 1.55 g C m^{-2} d^{-1}, and 3.19 g C m^{-2} d^{-1}, measured average daily R_h, R_a and R_{eco} were within the range of values reported for winter wheat by *Demyan* et al. (2016), *Prolingheuer* et al. (2014), and *Zhang* et al. (2013).

Observed R_a and R_h were in general smaller than the independently measured R_{eco}, contributing in average 58% and 42% to R_{eco} (Fig. 2), showing a lower contribution of R_a to R_{eco} compared to *Suleau* et al. (2011) and *Moureaux* et al. (2008), who reported a ratio of 76% to 24% and 79% to 21%, respectively. This might be explained by temporal dynamics of R_{eco} and its flux components, altering the contribution of R_a and R_h to overall R_{eco} throughout the season.

Hence, the lower contribution of R_a to R_{eco} found in this study is most likely due to the long and distinct period of senescence during the end of the reproductive plant phenological stage. However, when calculating the contribution of R_a and R_h to R_{eco} from beginning of December to beginning of July, the contribution of R_a (70%) and R_h (30%) becomes similar to ratios reported in the literature (*Moureaux* et al., 2008; *Suleau* et al., 2011).

Seasonal contributions of $R_{a\ (root)}$ (32%) and $R_{a\ (shoot)}$ (67%) to R_a were less distinct compared to ratios given by *Suleau* et al. (2011), who reported a higher contribution of 78% of $R_{a\ (shoot)}$ to R_a for winter wheat, but similar to the ratio found by *Moureaux* et al. (2008). In addition, the contribution of $R_{a\ (root)}$ (28%) to the total soil CO_2 efflux (R_{soil}) is comparable to *Prolingheuer* et al. (2010; 31%) and *Zhang* et al. (2013; 36%). Figure 2 indicates that major growth of root biomass seems to occur during the late juvenile and early adult plant phenological stage, a development which was slightly ahead when compared to the growth of shoot biomass, which started early during May and ended in July. This is in accordance with *Munkholm* et al. (2008) and *Barraclough* (1984) who reported similar root and shoot growth dynamics for winter wheat. Hence, also the partition of $R_{a\ (total)}$ into its above and below-

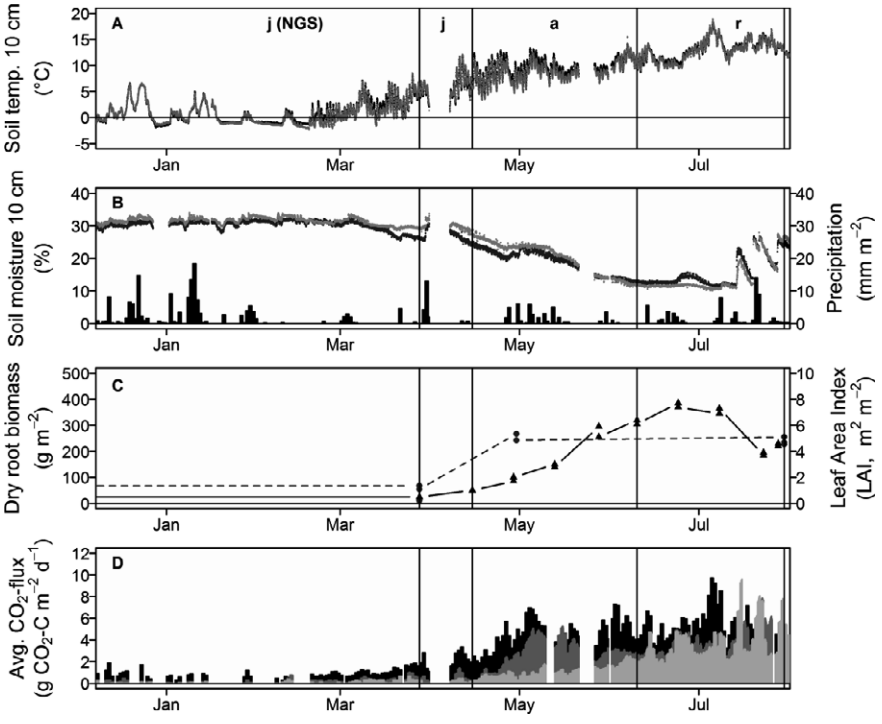

Figure 2: Time series of environmental conditions (A, B), above and belowground biomass development (C), and average of daily measured CO_2 flux (D) during the study period from beginning of December 2014 to end of July 2015. The juvenile (j), adult (a), and reproductive (r) plant phenological stages are marked by letters (A) and separated by vertical solid black lines. In addition the non-growing season period is indicated (NGS) Chart A and B are representing soil temperature and moisture in 10 cm depth for the root exclusion plot (dots; dark gray) and root inclusion plot (dots; black), respectively. Chart C shows the average LAI measured within the automatic chambers (triangles connected by solid line) and standing root biomass observed by mini-rhizotrons (circles connected by dashed line). Chart D shows the average of daily measured CO_2 flux measured by the AC system (R_{eco}; black) and its components measured at the root exclusion plot (R_h; light gray) and root inclusion plot (R_{soil}; dark gray).

© 2018 WILEY-VCH Verlag GmbH & Co. KGaA, Weinheim

Table 1: Average of daily measured R_{eco} and its flux components [$R_{a\ (total)}$, $R_{a\ (root)}$, $R_{a\ (shoot)}$ and R_h] ± SD for the juvenile, adult and reproductive plant phenological stage as well as the entire study period. In addition, potential environmental drivers are given.

Time period	Crop phenology	R_{eco}	R_h	R_a				Precipitation		GWL	Soil moisture in 10 cm depth	Temperature		LAI	Root biomass	
				Total	Shoot	Root	Shoot	Root	Sum	Daily			Air in 20 cm	Soil in 10 cm		Growth	Decay
		($g\ C\ m^{-2}\ d^{-1}$)					(%)		(mm)	($mm\ d^{-1}$)	(cm)	(vol.-%)	(°C)			($g\ cm^{-3}$ soil)	
2014–2015	Juvenile[a]	1.2 ± 0.7	0.2 ± 0.2	1.0 ± 0.7	0.8 ± 0.6	0.2 ± 0.2	80	20	186	1.4	54 ± 31	30 ± 2.4	3.1 ± 4.3	1.3 ± 2.7	1	0.007	0.000
	Adult[b]	4.6 ± 1.7	1.1 ± 0.5	3.3 ± 1.3	1.7 ± 1.1	1.6 ± 1.3	51	49	41	0.7	81 ± 16	20 ± 4.4	11.2 ± 4.9	9.1 ± 1.9	6.25	0.409	0.005
	Reproductive[c]	5.3 ± 2.0	3.7 ± 1.5	1.5 ± 2.1	1.4 ± 1.9	0.1 ± 1.3	94	6	79	1.5	156 ± 28	15 ± 4.9	16.7 ± 5.3	12.9 ± 1.9	4.5	0.029	0.051
Study period		3.2	1.3	1.7	1.2	0.6	68	32	306	1.3	83	24	8.0	5.7	–	0.445	0.056

[a]before 15.04.2015;
[b]15.04 to 10.06.2015;
[c]after 10.06.2015.

ground components $R_{a\ (shoot)}$ and $R_{a\ (root)}$ is highly variable and changes throughout the crop season (*Suleau* et al., 2011). The contribution of $R_{a\ (root)}$ to $R_{a\ (total)}$ was highest during the period of intense root development within the adult phenological stage (49%) and significantly lower during the juvenile (20%) and reproductive phenological stage (6%), respectively. The former can be explained by the minor amount of root biomass present at the measurement site, the latter by reaching senescence during maturity. However, the decrease of R_a during the reproductive plant phenological stage (*e.g.*, *Moureaux* et al., 2008) seemed to be compensated by the increase of R_h due to higher soil temperatures and enhanced soil moisture during the end of the crop season, resulting in a constant R_{eco} flux from beginning of May to end of July 2015 (Figs. 2 and 3; Tab. 1).

In general R_{eco} fluxes followed the observed temperature regime and were closely connected to plant growth (Fig. 2; Tab. 2). As a result of this, the highest R_{eco} fluxes of the study period were observed during the first half of July, when temperature as well as LAI culminated (Figs. 2 and 3). The dependency of R_{eco} on temperature and living biomass is well documented in literature (*e.g.*, *Lloyd* and *Taylor*, 1994; *Suleau* et al., 2011). Soil temperature and moisture directly affect microbial (R_h) as well as plant physiological activity, thus influencing the mineralization rate of organic materials and plant biochemical processes, respectively (*Reichstein* et al., 2005). In addition, plant respiration (R_a) is correlated with the amount of living above and belowground biomass, with higher plant respiration resulting from larger amounts of biomass (Tab. 2). This is in accordance with *Prolingheuer* et al. (2010) and *Moureaux* et al. (2008), who measured highest rhizospheric respiration rates for winter wheat during periods of massive plant growth.

As a result, R_a and R_h both respond to environmental drivers, *i.e.*, soil temperature and moisture (*Suleau* et al., 2011; *Zhang* et al., 2013), but only R_a responds to plant development (Tab. 2; Fig. 3; *Zhang* et al., 2013). Figure 3 shows that R_h follows soil temperature and soil moisture in 10 cm depth, whereas $R_{a\ (root)}$ increases with increasing root biomass (Figs. 2 and 3; Tab. 1). $R_{a\ (shoot)}$ responds well to biweekly measurements of LAI as a proxy for plant/biomass development (Tab. 1).

3.2 Methodological improvements and limitations

Measuring R_{eco} and its components by combining a root exclusion experimental setup with measurements from automatic chambers and soil CO_2 sampling tubes has three major advantages. First, it allows for the separation of R_{eco} into R_a and R_h by comparing fluxes resulting from the root exclusion (R_h) and root inclusion (R_{eco} and R_{soil}) plot (Fig. 1). Second, the influence of plot-scale soil heterogeneity could be excluded during future studies by operating both measurement devices on the same pedon. As a result and given a sufficient number of repetitions, it would allow not only to investigate temporal, but also spatial dynamics of R_{eco}, R_a and R_h. Third, determining the CO_2 fluxes by two complementary measurement devices (above and belowground) may help to overcome measurement system specific limitations, such as

© 2018 WILEY-VCH Verlag GmbH & Co. KGaA, Weinheim

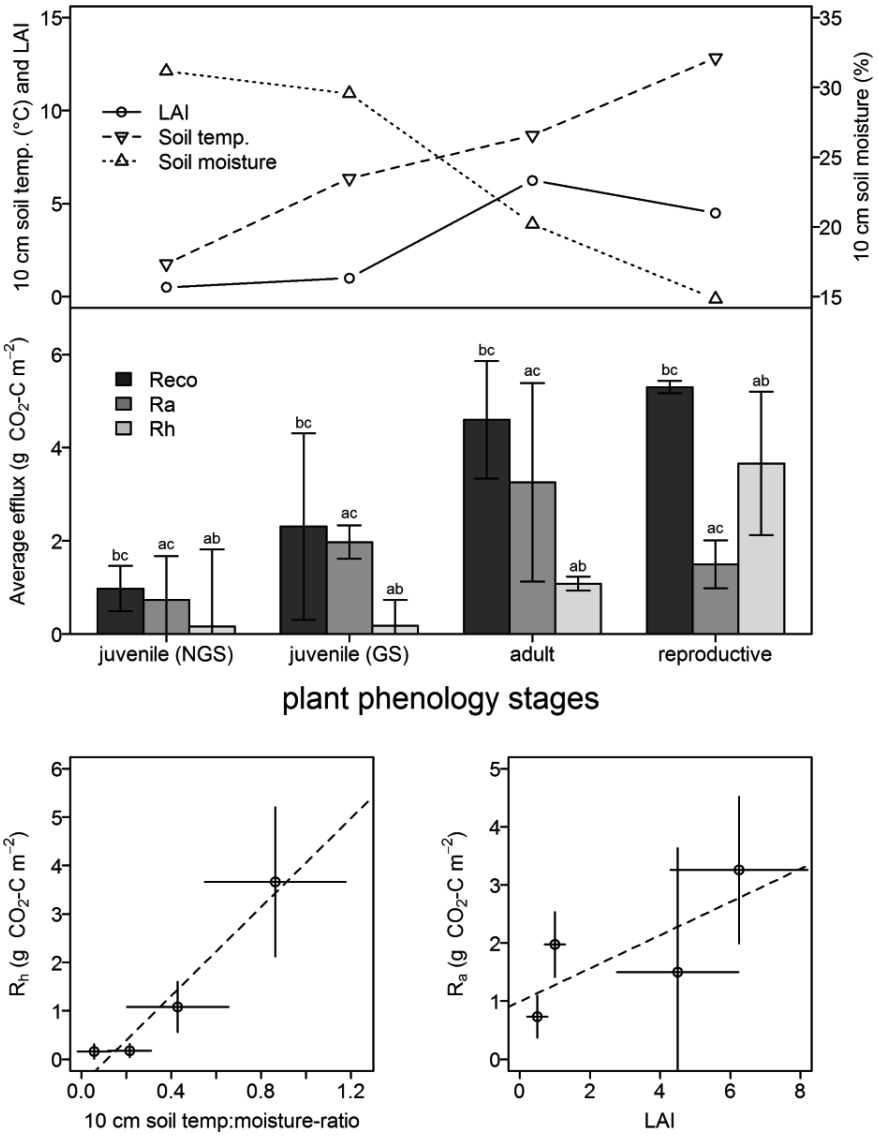

Figure 3: Average measured R_{eco} and R_h as well as calculated R_a fluxes during the juvenile, adult and reproductive plant phenological stage. Error bars represent the ± 1 SD of measured fluxes. Small letters indicate significant differences between R_{eco}, R_a and R_h fluxes measured during one phenological stage. The dependencies of average values (plant phenology stages) of R_a and R_h from LAI (circles; dashed black line) and soil temperature (triangle; solid black line) and soil moisture (triangle;dotted black line), respectively, are shown.

measurements during storm or ground frost, when AC measurements are impossible due to strong wind or freezing of the chamber on the frame, but belowground CO_2 concentration measurements still allow for estimating R_{soil}. In reverse, AC measurements may help to capture the response of R_{eco} to management activities such as tillage, based on their faster and easier setup. As a result, short-term peaks in soil respiration which can substantially contribute to R_{eco}, such as after tillage, heavy rain events or during frost-thaw cycling might be identified.

However, both measurement devices, the subsequent flux determination as well as the assumptions made to separate R_{eco} into its components, introduced a number of potential error sources. AC measurements and the derived R_{eco} fluxes might be biased due to ecophysiological disturbances induced by chamber deployment, such as the alteration within chamber air temperature, humidity, pressure, solar radiation and gas concentration gradient (*Kutzbach* et al., 2007; *Lai* et al., 2012; *Langensiepen* et al., 2012). However, by reducing the chamber deployment time to a minimum and accounting for changes in environmental conditions during data processing and flux calculation, the influence of the mentioned disturbances can be minimized (*Hoffmann* et al., 2015). Based on the transparent chambers used in our approach, the calculated R_{eco} fluxes as well as R_{soil} and R_h fluxes compared against R_{eco} are solely based on nighttime measurements. Hence, systematic differences between nighttime and daytime R_{eco}, due to, *e.g.*, crop phenology driven differences in R_a are not detectable.

Table 2: Standardized beta coefficients and significance level of linear regressions for R_{eco} and its flux components with potential environmental drivers during the juvenile (j), adult (a) and reproductive (r) plant phenological stage, respectively.

CO_2 flux	Soil temp. in 10 cm			Soil moisture in 10 cm			Dry root biomass			LAI		
	j	a	r	j	a	r	j	a	r	j	a	r
	(°C)			(Vol.-%)			(g m^{-2})			(m^{-2} m^{-2})		
R_{eco}	0.80***	0.59***	0.71***	–0.72***	–0.31***	–0.28***	0.64***	0.56***	0.10·	0.63***	0.35***	0.27***
R_h	0.04	0.76***	0.05	–0.1*	–0.95***	–0.66***	not applicable					
R_a	0.50***	0.02	0.63***	–0.43***	0.35***	0.29***	0.41***	0.21***	–0.43***	0.40***	–0.34***	–0.44***
$R_{a\ (shoot)}$	0.67***	0.03	0.57***	–0.54***	0.42***	0.33***	0.51***	–0.21***	–0.36***	0.48***	–0.47***	–0.32***
$R_{a\ (root)}$	–0.1**	–0.01	0.05	0.07·	–0.1*	–0.06	–0.07·	0.60***	0.69	–0.04	0.20***	–0.13*

© 2018 WILEY-VCH Verlag GmbH & Co. KGaA, Weinheim

The flux determination based on belowground CO_2 concentration measurements offers several advantages, such as the possibility for spatially distinct, continuous *in situ* measurements, disregarding certain weather conditions, which affect aboveground CO_2 concentration measurements. However, there are also a number of disadvantages, including initial soil disturbance due to installation, difficulties with placement of tubing near the soil surface and problems with impounding water or water vapor (*DeSutter* et al., 2008). The root exclusion experimental setup is in general assumed to be suitable for croplands, although it is related to difficulties when, *e.g.*, implemented in forest or grassland ecosystems (*Kuzyakov* and *Larionova*, 2005). Even though the implementation of the root exclusion plot induced differences in the microclimatological conditions, differences found in soil temperature and soil moisture were insignificant (paired t-test; p-value ≤ 0.1) with maximum differences of 1.4°C and 7.5% which are much lower compared to values reported by *Suleau* et al. (2011) for a larger (3 m × 3 m) root exclusion area. In average, the root exclusion plot was 0.9% wetter and 0.2°C colder compared to the root inclusion plot. Additionally, the root exclusion plot was directly exposed to rain and no roots were present, thus soil surface was susceptible to silting and soil structure was prone to compaction or hard setting in a much higher degree as compared to the root inclusion plot. Consequently, gas diffusion and exchange with the above ground atmosphere might decrease or even be blocked at particular times. In addition, trenches inserted down to 30 cm soil depth at the fallow plot might be insufficient to prevent lateral ingrowth of roots or root respiration originating from deeper soil layers for R_h measurements. Besides of these measurement systems related error sources, the partitioning of R_{eco} might also be biased due to differences in soil properties, as well as differences regarding root growth and microbial activities, either induced by the experimental setup (*Subke* et al., 2006; *Kuzyakov* and *Larionova*, 2005; *Hanson* et al., 2000) or as a result of small-scale spatial heterogeneity. This error source, however, might only be reduced by implementing a sufficient number of repetitions for both, chamber as well as soil tube measurement plots.

3.3 Implications for R_{eco} partitioning of croplands

To overcome the mentioned limitations and using the presented flux separation approach for a sufficient separation of *in situ* measurements of R_{eco} into its components R_a and R_h, a number of implications have to be considered:

(1) In accordance with *Subke* et al. (2006) and *Hanson* et al. (2000), measurements of CO_2 efflux should not start immediately after installation of the belowground CO_2 concentration measurement system. Even though the root exclusion plot did not contain dying root biomass as trenched plots would have, burying of wire cloth and gas sampling tubes introduced substantial disturbances to the upper soil horizons. Consequently, it is recommended to allow for re-equilibration to steady state soil conditions prior to belowground CO_2 concentration measurements (*Hanson* et al., 2000). However, this problem is of minor relevance for croplands, where the installation of the measurement device falls together with large-scale disturbance of the top soil layer due to tillage anyway.

(2) Depending on the type of the investigated cover crop (*e.g.*, perennial plants), it might be needed to extend the root exclusion to deeper soil layers in order to prevent ingrowth of roots and, thus, contributions from root respiration to R_h. This should ideally be escorted by a non-destructive monitoring of root growth.

(3) As an alternative to sampling tubes, soil gas probes could be installed in the center of the root exclusion plot to minimize fringe effects. However, while probes are rather an isolated sampling device, tubes provide gas samples integrated across a soil volume around the 4 m tube length.

(4) In addition, the size of the root exclusion plot should be kept as small as possible to minimize environmental impacts (temperature increase through direct solar radiation, silting and soil compaction due to rain, *etc*.), but large enough to prevent effects of lateral CO_2 diffusion from adjacent pedons.

(5) Above and belowground CO_2 concentration measurements should be performed at the same pedon to eliminate the bias based on present plot-scale spatial heterogeneity.

(6) To detect changes in the contribution of $R_{a\ (root)}$, $R_{a\ (shoot)}$ to $R_{a\ (total)}$ and thus R_{eco}, as well as to determine environmental drivers, the measurement should cover the entire crop season.

(7) To measure the diurnal variability of R_{eco} and thus investigate whether above or belowground R_a fluxes differ systematically between day and night, the experimental setup could be accompanied by an opaque AC system, allowing for daytime R_{eco} measurements.

(8) In addition, isotopic approaches should be included within the experimental setup. By combining the AC system with, *e.g.*, ^{13}C or ^{14}C labeling approaches, the NPP and the input of plant-based C might be quantified. Moreover, assessing the ^{13}C or ^{14}C natural abundance might help to avoid limitations of the root exclusion method, whereas measurements of CO_2 exchange by using the AC or soil CO_2 sampling system might make up for some of the weaknesses of the isotopic approaches (*Kuzyakov*, 2006; *Paterson* et al., 2009; *Hopkins* et al., 2013).

4 Conclusions

The presented approach of a pin-point separation of R_{eco} using a combination of automatic chamber and soil tube measurements together with a root exclusion experimental setup showed reasonable results. R_{eco} as well as its components $R_{a\ (root)}$, $R_{a\ (shoot)}$ and R_h were within the range of values reported for winter wheat by literature. In addition, automatic CO_2 flux measurements of both systems, allowed to reveal temperature and plant phenology related temporal dynamics within the contribution of $R_{a\ (root)}$ and $R_{a\ (shoot)}$ to R_a, as well as of R_a and R_h to overall R_{eco}. Based on these dynamics, the contribution of R_h and R_a to seasonal R_{eco}, differs depending on the length of plant development stages, such as the length of senescence during the end of the reproductive stage.

To enhance the accuracy of the proposed approach for R_{eco} flux separation and to reduce the bias due to small-scale spatial heterogeneity, measurements of R_{eco} and R_{soil} should be performed at the same spatial entity, a setup only possible by using the presented combination of automatic chamber and

© 2018 WILEY-VCH Verlag GmbH & Co. KGaA, Weinheim

soil CO_2 tube measurement systems. Regarding field scale estimates of different flux components, the number of repetitions should be increased in future studies to enhance precision of measurements.

Acknowledgment

This work was supported by the *Brandenburg Ministry of Infrastructure and Agriculture* (*MIL*), who financed land purchase, the *Federal Agency for Renewable Resources* (*FNR*), who co-financed the AC system, and the interdisciplinary research project *CarboZALF*. We thank *Gernot Verch* and all employees of the ZALF research station Dedelow, for cultivation and support at the CarboZALF-D field trial. Special thanks go to *Marten Schmidt, Peter Rakowsk*i and *Dieter Sowa* for excellent operational and technical maintenance of used measurement devices during the study period. The authors thank *Katja Kühdorf* and *Anne-Katrin Prescher* for proof reading.

References

Barraclough, P. B. (1984): The growth and activity of winter wheat roots in the field: root growth of high-yielding crops in relation to shoot growth. *J. Agric. Sci.* 103, 439–442.

Batjes, N. H., *van Wesemael, B.* (2015): Measuring and Monitoring Soil Carbon, in Banwart, S. A., Noellemeyer, E., Milne, E. (eds.): Soil Carbon: Science, Management and Policy for Multiple Benefits. SCOPE Series 71. CABI, Wallingford, UK, pp. 188–201.

Batjes, N. H. (1996): Total carbon and nitrogen in the soils of the world. *Eur. J. Soil Sci.* 47, 151–163.

Bhupinderpal-Singh, *Nordgren, A.*, *Löfvenius, M. O.*, *Högberg, M. N.*, *Mellander, P.-E.*, *Högberg, P.* (2003): Tree root and soil heterothropic respiration as revealed by girdling of boreal Scots pine forests: extending observations beyond the first year. *Plant Cell Environ.* 26, 1287–1296.

Bond-Lamberty, B., *Wang, C.*, *Gower, S. T.* (2004): A global relationship between the heterothropic and autotrophic components of soil respiration. *Global Change Biol.* 10, 1756–1766.

Chen, L., *Smith, P.*, *Yang, Y.* (2015): How has soil carbon stock changed over recent decades? *Global Change Biol.* 21, 3197–3199.

DeSutter, T. M., *Sauer, T. J.*, *Parkin, T. B.*, *Heitman, J. L.* (2008): A subsurface, closed-loop system for soil carbon dioxide and its application to the gradient efflux approach. *Soil Sci. Soc. Am. J.* 72, 126–134.

Demyan, M. S., *Ingwersen, J.*, *Nkwain Funkuin, Y.*, *Shahbaz Ali, R.*, *Mirzaeitalarposhti, R.*, *Rasche, F.*, *Poll, C.*, *Müller, T.*, *Streck, T.*, *Kandeler, E.*, *Cadisch, G.* (2016): Partitioning of ecosystem respiration in winter wheat and silage maize—modeling seasonal temperature effects. *Agric. Ecosyst. Environ.* 224, 131–144.

Eglin, T., *Ciais, P.*, *Piao, S. L.*, *Barre, P.*, *Bellassen, V.*, *Cadule, P.*, *Chenu, C.*, *Gasser, T.*, *Koven, C.*, *Reichstein, M.*, *Smith, P.* (2010): Historical and future perspectives of global soil carbon response to climate and land-use changes. *Tellus B* 62, 700–718.

Hanson, P. J., *Edwards, N. T.*, *Garten, C. T.*, *Andrews, J. A.* (2000): Separating root and soil microbial contribution to soil respiration: a review of methods and observations. *Biogeochem.* 48, 115–146.

Hoffmann, M., *Jurisch, N.*, *Albiac Borraz, E.*, *Hagemann, U.*, *Drösler, M.*, *Sommer, M.*, *Augustin, J.* (2015): Automated modeling of ecosystem CO_2 fluxes based on periodic closed chamber measurements: a standardized conceptual and practical approach. *Agric. For. Meteorol.* 200, 30–45.

Hoffmann, M., *Jurisch, N.*, *Garcia Alba, J.*, *Albiac Borraz, E.*, *Schmidt, M.*, *Huth, V.*, *Rogasik, H.*, *Verch, G.*, *Sommer, M.*, *Augustin, J.* (2017): Detecting small-scale spatial heterogeneity and temporal dynamics of soil organic carbon (SOC) stocks: a comparison between automatic chamber-derived C budgets and repeated soil inventories. *Biogeosciences* 14, 1003–1019.

Hopkins, F., *Gonzalez-Meler, M. A.*, *Flower, C. E.*, *Lynch, D. J.*, *Czimczik, C.*, *Tang, J.*, *Subke, J.-A.* (2013): Ecosystem-level controls on root-rhizosphere respiration. *New Phytol.* 199, 339–351.

IUSS Working Group WRB (2015): World Reference Base for Soil Resources 2014, update 2015, International soil classification system for naming soils and creating legends for soil maps. World Soil Resources Reports No. 103. FAO, Rome, Italy.

Jones, H. G. (1992): Plant and Microclimate: A Quantitative Approach to Environmental Plant Physiology. Cambridge University Press, New York, NY, USA.

Kutzbach, L., *Schneider, J.*, *Sachs, T.*, *Giebels, M.*, *Nykanen, H.*, *Shurpali, N. J.*, *Martikainen, P. J.*, *Alm, J.*, *Wilmking, M.* (2007): CO_2 flux determination by closed-chamber methods can be seriously biased by inappropriate application of linear regression. *Biogeosciences* 4, 1005–1025.

Kuzyakov, Y., *Larionova, A. A.* (2005): Root and rhizomicrobial respiration: a review of approaches to estimate respiration by autothrophic and heterothrophic organisms in soil. *J. Plant Nutr. Soil Sci.* 168, 503–520.

Kuzyakov, Y. (2006): Sources of CO_2 efflux from soil and review of partitioning methods. *Soil Biol. Biochem.* 38, 425–448.

Lai, D. Y. F., *Roulet, N. T.*, *Humphreys, E. R.*, *Moore, T. R.*, *Dalva, M.* (2012): The effect of atmospheric turbulence and chamber deployment period on autochamber CO_2 and CH_4 flux measurements in an ombothrophic peatland. *Biogeosciences* 9, 3305–3322.

Lal, R., *Griffin, M.*, *Apt, J.*, *Lave, L.*, *Morgan, M. G.* (2004): Managing soil carbon. *Science* 304, 393–393.

Lancashire, P. D., *Bleiholder, H.*, *van den Boom, T.*, *Langelüddeke, P.*, *Stauss, R.*, *Weber, E.*, *Witzenberger, A.* (1991): A uniform decimal code for growth stages of crops and weeds. *Ann. Appl. Biol.* 119, 561–601.

Langensiepen, M., *Kupisch, M.*, *van Wijk, M. T.*, *Ewert, F.* (2012): Analyzing transient closed chamber effects on canopy gas exchange for flux calculation timing. *Agric. For. Meteorol.* 164, 61–70.

Leiber-Sauheitl, K., *Fuß, R.*, *Voigt, C.*, *Freibauer, A.* (2014): High greenhouse gas fluxes from grassland on histic gleysol along soil C and drainange grasslands. *Biogeosciences* 11, 749–761.

Livingston, G. P., *Hutchinson, G. L.* (1995): Enclosure-Based Measurement of Trace Gas Exchange: Applications and Sources of Error, in Matson, P. A., Harris, R. C. (eds.): Methods in ecology. Biogenic trace gases: Measuring emissions from soil and water. Blackwell Science, Hoboken, NJ, USA, pp. 14–51.

Lloyd, J., *Taylor, J. A.* (1994): On the temperature dependence of soil respiration. *Funct. Ecol.* 8, 315–323.

Lugato, E., *Bampa, F.*, *Panagos, P.*, *Montanarella, L.*, *Jones, A.* (2014): Potential carbon sequestration of European arable soils estimated by modelling a comprehensive set of management practices. *Global Change Biol.* 20, 3557–3567.

Luo, Y., *Ahlström, A.*, *Allison, S. D.*, *Batjes, N. H.*, *Brovkin, V.*, *Carvalhais, N.*, *Chappell, A.*, *Ciais, P.*, *Davidson, E. A.*, *Finzi, A.*, *Georgiou, K.*, *Guenet, B.*, *Hararuk, O.*, *Harden, J. W.*, *He, Y.*, *Hopkins, F.*, *Jiang, L.*, *Koven, C.*, *Jackson, R. B.*, *Jones, C. D.*,

© 2018 WILEY-VCH Verlag GmbH & Co. KGaA, Weinheim

Lara, M. J., *Liang, J.*, *McGuire, D.*, *Parton, W.*, *Peng, C.*, *Randerson, J. T.*, *Salazar, A.*, *Sierra, C. A.*, *Smith, M. J.*, *Tian, H.*, *Todd-Brown, K. E. O.*, *Torn, M.*, *van Groenigen, K. J.*, *Wang, Y. P.*, *West, T. O.*, *Wei, Y.*, *Wieder, W. R.*, *Xia, J.*, *Xu, X.*, *Xu, X.*, *Zhou, T.* (2015): Towards more realistic projections of soil carbon dynamics by earth system models. *Global Biogeochem. Cy.* 30, 40–56.

Moldrop, P., *Olesen, T.*, *Yamaguchi, T.*, *Schonning, P.*, *Rolaton, D. E.* (1999): Modeling diffusion and reation in soils IX. The Buckingham-Burdine-Campbell equation for gas diffusivity in undisturbed soil. *Soil Sci.* 164, 542–551.

Moureaux, C., *Debacq, A.*, *Hoyaux, J.*, *Suleau, M.*, *Tourneur, D.*, *Vancutsem, F.*, *Bodson, B.*, *Aubinet, M.* (2008): Carbon balance assessment of a Belgian winter wheat crop (*Triticum aestivum* L.). *Global Change Biol.* 14, 1353–1366.

Munkholm, L. J., *Hansen, E. M.*, *Olesen, J. E.* (2008): The effect of tillage intensity on soil structure and winter wheat root/shoot growth. *Soil Use Manage.* 24, 392–400.

Myklebust, M. C., *Hipps, L. E.*, *Ryel, R. J.* (2008): Comparison of eddy covariance, chamber, and gradient methods of measuring soil CO_2 efflux in an annual semi-arid grass, *Bromus tectorum*. *Agric. For. Meteorol.* 148, 1894–1907.

Paterson, E., *Midwood, A. J.*, *Millard, P.* (2009): Through the eye of the needle: a review of isotope approaches to quantify microbial processes mediating soil carbon balance. *New Phytol.* 184, 19–33.

Pohl, M., *Hoffmann, M.*, *Hagemann, U.*, *Giebels, M.*, *Albiac Borraz, E.*, *Sommer, M.*, *Augustin, J.* (2015): Dynamic C and N stocks—key factors controlling the C gas exchange of maize in a heterogeneous peatland. *Biogeosciences* 12, 2737–2752.

Prolingheuer, N., *Scharnagl, B.*, *Graf, A.*, *Vereecken, H.*, *Herbst, M.* (2014): On the spatial variation of soil rhizospheric and heterotrophic respiration in a winter wheat stand. *Agric. For. Meteorol.* 195, 24–31.

Prolingheuer, N., *Scharnagl, B.*, *Graf, A.*, *Vereecken, H.*, *Herbst, M.* (2010): Spatial and seasonal variability of heterotrophic and autotrophic soil respiration in a winter wheat stand. *Biogeosci. Discuss.* 7, 9137–9173.

Reichstein, M., *Falge, E.*, *Baldocchi, D.*, *Papale, D.*, *Aubinet, M.*, *Berbigier, P.*, *Bernhofer, C.*, *Buchmann, N.*, *Gilmanov, T.*, *Granier, A.*, *Grünwald, T.*, *Havránková, K.*, *Ilvesniemi, H.*, *Janous, D.*, *Knohl, A.*, *Laurila, T.*, *Lohila, A.*, *Loustau, D.*, *Matteucci, G.*, *Meyers, T.*, *Miglietta, F.*, *Ourcival, J.-M.*, *Pumpanen, J.*, *Rambal, S.*, *Rotenberg, E.*, *Sanz, M.*, *Tenhunen, J.*, *Seufert, G.*, *Vaccari, F.*, *Vesala, T.*, *Yakir, D.*, *Valentini, R.* (2005): On the separation of net ecosystem exchange into assimilation and ecosystem respiration: review and improved algorithm. *Global Change Biol.* 11, 1424–1439.

Schrumpf, M., *Schulze, E. D.*, *Kaiser, K.*, *Schumacher, J.* (2011): How accurately can soil organic carbon stocks and stock changes be quantified by soil inventories? *Biogeosciences* 8, 1193–1212.

Smith, P., *Lanigan, G.*, *Kutsch, W. L.*, *Buchmann, N.*, *Eugster, W.*, *Aubinet, M.*, *Ceschia, E.*, *Béziat, P.*, *Yeluripati, J. B.*, *Osborne, B.*, *Moors, E. J.*, *Brut, A.*, *Wattenbach, M.*, *Saunders, M.*, *Jones, M.* (2010): Measurements necessary for assessing the net ecosystem carbon budget of croplands. *Agric. Ecosyst. Environ.* 139, 302–315.

Sommer, M., *Augustin, J.*, *Kleber, M.* (2016): Feedbacks of soil erosion on SOC patterns and carbon dynamics in agricultural landscapes—The CarboZALF experiment. *Soil Till. Res.* 156, 182–184.

Subke, J.-A., *Inglima, I.*, *Francesca Cotrufo, M.* (2006): Trends and methodological impacts in soil CO_2 efflux partitioning: a metaanalytical review. *Global Change Biol.* 12, 921–943.

Suleau, M., *Moureoux, C.*, *Dufranne, D.*, *Buysse, P.*, *Bodson, B.*, *Destain, J.-P.*, *Heinesch, B.*, *Debacq, A.*, *Aubinet, M.* (2011): Respiration of three Belgian crops: Partitioning of total ecosystem respiration in its heterothrophic, above- and below-ground autothrophic components. *Agric. For. Meteorol.* 151, 633–643.

Tang, J., *Misson, L.*, *Gershenson, A.*, *Cheng, W.*, *Goldstein, A. H.* (2005): Continous measurements of soil respiration with and without roots in a ponderosa pine plantation in the Sierra Nevada Mountains. *Agric. For. Meteorol.* 132, 212–227.

Van Oost, K., *Quine, T. A.*, *Govers, G.*, *De Gryze, S.*, *Six, J.*, *Harden, J. W.*, *Ritchie, J. C.*, *McCarty, G. W.*, *Heckrath, G.*, *Kosmas, C.*, *Giraldez, J. V.*, *da Silva, J. R.*, *Merckx, R.* (2007): The impact of agricultural soil erosion on the global carbon cycle. *Science* 318, 626–629.

Zhang, Q., *Lei, H.*, *Yang, D.* (2013): Seasonal variations in soil respiration, heterotrophic respiration and autothrophic respiration of a wheat and maize rotation cropland in the North China Plain. *Agric. For. Meteorol.* 180, 34–43.

© 2018 WILEY-VCH Verlag GmbH & Co. KGaA, Weinheim